**Supporting Information**

# Metasurface-dressed two-dimensional on-chip waveguide for free-space light field manipulation

*Yimin Ding,*[†‡] *Xi Chen,*[†‡] *Yao Duan,*[†‡] *Haiyang Huang,*[†‡] *Lidan Zhang,*[†] *Shengyuan Chang,*[†] *Xuexue Guo,*[†] *and Xingjie Ni*[†₴*]

[†] Department of Electrical Engineering, The Pennsylvania State University, University Park, PA 16802, USA.

[₴] Material Research Institute, Pennsylvania State University, University Park, PA 16802, USA.

[‡] These authors contributed equally.

[*] *Corresponding author:* *xingjie@psu.edu*

Number of pages: 5

Number of figures: 4

## 1. Device fabrication

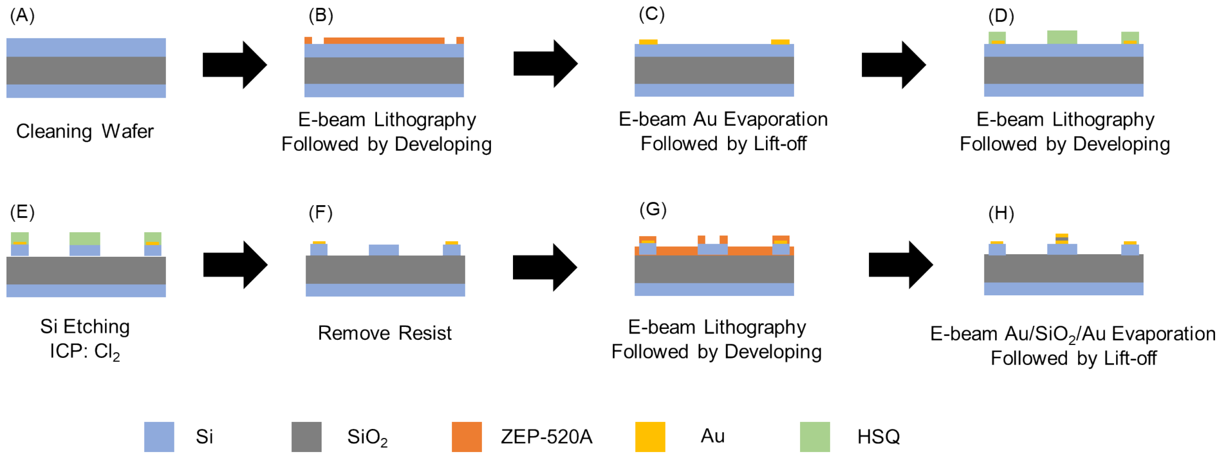

Figure. S1. An illustration of the fabrication process. (A) wafer cleaning by acetone and isopropanol, (B) spinning ZEP-520A resist, e-beam writing for alignment markers and development, (C) E-beam evaporation of Au and lift off, (D) defining waveguide by spinning HSQ resist, e-beam writing and development, (E) ICP dry etch by $Cl_2$ plasma, (F) removing HSQ by BOE wet-etching, (G) spinning ZEP-520A resist, e-beam writing for antennas and development, (H) E-beam evaporation of Au/$SiO_2$/Au trilayers and lift off, (I) The device is finally diced along with the input ports.

The samples were fabricated on a commercially available silicon-on-insulator wafer with 220-nm-thick (for beam steering experiments) and 500-nm-thick (for light focusing experiments) Si device layer and 3-µm buried silicon dioxide. The wafer was cleaned by sonication in acetone and IPA for 3 minutes, respectively. The alignment marker was defined by electron beam lithography with 100 kV beam (Vistec EBPG5200) followed by evaporation of 50 nm Au with a 5-nm-thick Ti adhesion layer (Kurt J. Lesker Lab-18) and lift-off. Then negative resist Fox-16 (Dow Corning Corp.) was spin-coated and prebaked at 100 °C for 4 minutes. The waveguide pattern was written, followed by development in CD-26 developer (MicroChem) for 25 minutes to reduce the proximity effect. Chlorine-based inductively coupled reactive ion etching (ICP-RIE) was used to etch crystalline Si with FOX-16 resist as a mask (Plasma-Therm Versalock 700). The sample was immersed in buffered oxide etchant for 20 seconds, followed by a water rinse to remove the remaining mask. ZEP 520A (Zeon) was spin-coated on the sample and soft-baked at 180 °C for 3 minutes. A second-step electron beam lithography was conducted to define the metasurface layer on top of the waveguide with precise alignment. The exposed sample was developed in N-amyl-acetate for 3 minutes, followed by MIBK:IPA immersion for 1 minute. Au/SiO2/Au films were subsequently deposited using an electron beam evaporation system (Semicore). The pattern was lifted off in 1165 remover (MicroChem) at 85 °C in a water bath for 2 hours. The sample was finally diced along the input ports of the waveguide for measurement.

## 2. Design of the meta-atoms

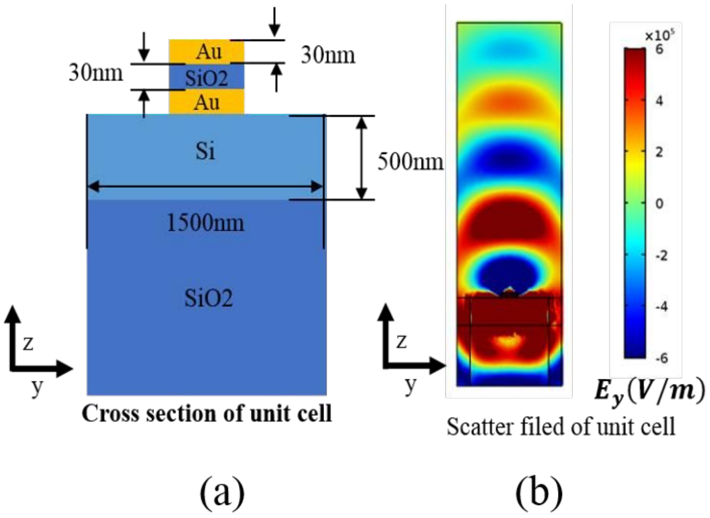

Figure. S2 (a) The unit cell of metasurface element on silicon waveguide. The silicon rectangular waveguide is 1500nm*500nm, and the two-gold layer is 30nm and the silicon dioxide layer is 30nm. (b) The scattered electric field of the meta-atoms.

The proposed metal-insulator-metal sandwich structured meta-atoms (Figure. S2(a)) were simulated using COMSOL Multiphysics. The fundamental mode $TE_{00}$ excites the two resonances mode (ED and MD) of the nanoantenna. The nanoantenna scattered the light into the free space on the top layer (Figure. S2(b)).

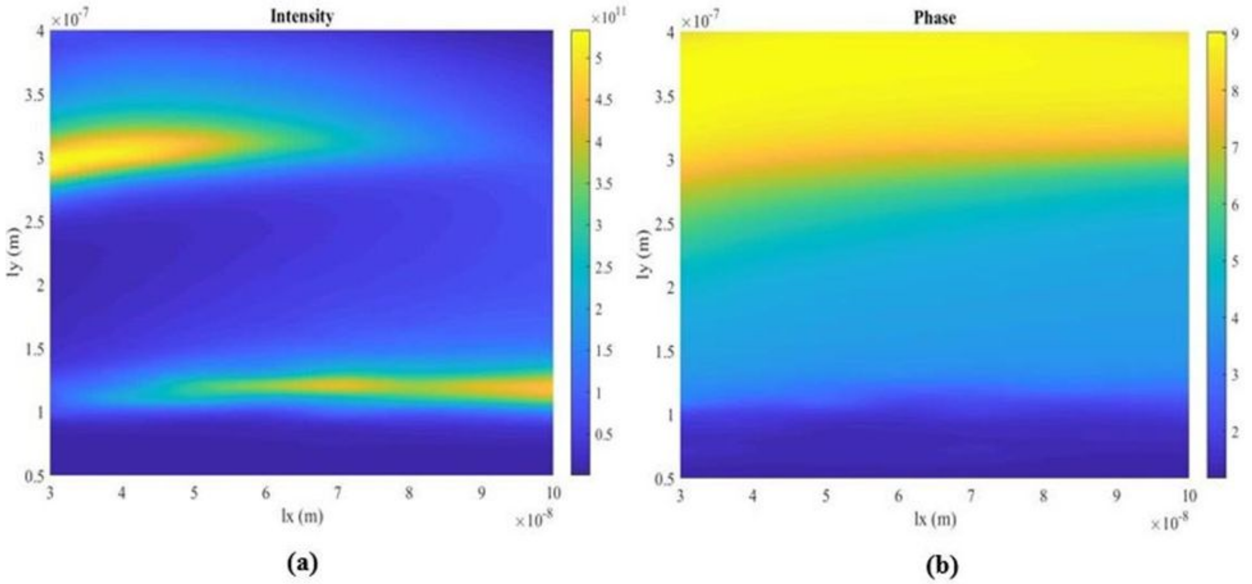

Figure. S3 The simulation result of unit cell designed on the top of silicon rectangular waveguide (a) intensity profile has two peaks around ly = 100nm and 300nm and (b) phase response from ly increasing, we can have the phase shift from 1 radiant to 9 radiant which is enough for covering total phase range.

The response from the nanoantenna has been calculated by a point monitor a few wavelengths above the center of the nanoantenna. The software allows us to extract the amplitude and phase information from it. So, first, we calculated the fundamental mode effective index of the 1550nm by 500nm silicon waveguide with operation wavelength 1550nm. Then we swept two dimensions of the nanoantenna ax and ay(length along x and y direction) so that we can have the complete picture of the optical response from the nanoantenna as we can find in Figure. S3. Figure. S3(b) shows that we can achieve 2π phase shift which is large enough for us to modulate the scattering light fully. However, due to the high wavelength sensitivity of the metasurfaces elements, we can also achieve different responses to the scattering light by incident signal with different wavelengths.

## 3. Design consideration on minimizing the distortion of guided was

In our designs, we keep the distortion to a negligible degree. The thickness of the waveguide was chosen to be sufficiently thin to avoid the existence of $TE_{x0}$ modes (high-order modes along the vertical direction), while also to be as thick as possible to minimize the impact from the meta-atoms. In addition, the period of the meta-atom array along propagation direction was designed to be 220 nm, smaller than a half wavelength of the guided wave to avoid the Bragg reflection. We validated our design using full-wave FDTD simulations. After the guided wave passes through a metasurface of 242 (11×22) meta-atoms, the purity of $TE_{00}$ mode is higher than 98.5%. Therefore, we can safely assume that the presence of each meta-atom has only a small perturbation to the guided modes.

## 4. Bandwidth analysis of the device

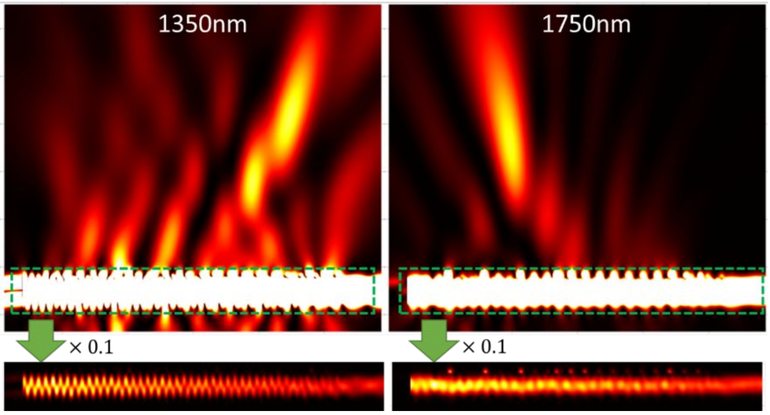

Figure. S4 Full-wave simulated intensity distribution of the designed metalens on a waveguide (the same design as shown in Figure 2 in the main text).

Our metalens can focus in a wavelength range of roughly 400 nm (1350 – 1750 nm), which is validated in our full-wave simulations. The focus spot moves along the waveguide due to the change of the guided wave's propagation constant (Figure. S4 top panels). In addition, high-order modes in a vertical direction begin to emerge in the shorter wavelength range, which deteriorates the focusing performance (Figure. S4 bottom panels).